Orthopositronium scattering off H and He

Simone Chiesa* and Massimo Mella[†]

Dipartimento di Chimica Fisica ed Elettrochimica, Università degli Studi di Milano, Via Golgi 19, 20133 Milano, Italy

Gabriele Morosi[‡]

Dipartimento di Scienze Chimiche, Fisiche e Matematiche, Università dell'Insubria, Via Lucini 3, 22100 Como, Italy

Exploiting an approach similar to the *R*-matrix theory, the diffusion Monte Carlo method is employed to compute phase shifts and threshold cross sections for the elastic scattering of positronium off light atoms. We briefly review the main ideas behind the use of quantum Monte Carlo techniques in scattering problems and, as applications, we present results for Ps-H and Ps-He. We find scattering lengths of 4.375(34) and 2.228(50) a.u. for the singlet and the triplet states of Ps-H, and of 1.4046(6) a.u. for Ps-He. A discussion of the agreement with other recent estimates for the same quantities is included. In particular, the scattering length for the Ps-H singlet agrees within 1% with the stochastic variational minimization (SVM) estimate by Ivanov, Varga, and Mitroy [Phys. Rev. A **65**, 32703 (2002)] and the *R*-matrix one by Blackwood, McAlinden, and Walter [Phys. Rev. A **65**, 32517 (2002)]. The Ps-H triplet scattering length, which still shows good agreement (1%) with the SVM one, appears to be 10% larger than the *R*-matrix value. As far as Ps-He is concerned, the calculation has been performed in a fully many-body framework. Comparison of the diffusion Monte Carlo scattering length with other estimates allows us to qualitatively and quantitatively assess the degree of approximation involved in other approaches.

I. INTRODUCTION

Positronium (Ps) scattering off atomic and molecular targets has overwhelming importance for understanding the interaction mechanism between an overthermal Ps and a condensed matter environment [1]. For instance, by means of elastic and inelastic cross sections, it is possible to model energy transfers from Ps to the surroundings or to describe the Ps trapping in a free volume cavity. Despite its long history [2–7], and even in the case of light atoms, some quantitative aspects of the process still remain controversial and have recently been addressed by a number of authors, both experimentally [8–11] and theoretically [12–16]. From the computational point of view, the difficulties that almost every method is faced with are related to the composite nature of both target and projectile. As a consequence, sensible results can be obtained only if correlation and exchange effects are properly treated. Moreover, when o-positronium is considered, the internal 2γ decay is symmetry forbidden and annihilation is likely to take place with one of the target electrons. This process, which is the dominant decay process when the system has an electronic closed shell, is called "pick-off" annihilation. For an accurate estimate of its rate, the correct treatment of the electron-positron correlation is fundamental.

A sound treatment of exchange and correlation has only recently been achieved for the case of positronium scattering off hydrogen and positronium atoms [17,14,18,19]. However, the full *ab initio* treatment (i.e., without the use of exchange or correlation model potentials) of systems with more than two electrons still represents a formidable task. For instance Ps-He has not been treated in a fully many-body framework. A glance at the recent literature on bound systems containing a positron reveals an essentially identical situation with only a small number of electrons treated explicitly. In this context, our group has shown [20] that flexible and accurate computational techniques for small and medium size systems are provided by the family of quantum Monte Carlo (QMC) methods. Among them, the diffusion Monte Carlo (DMC) scheme represents the most powerful approach to studying strongly correlated systems thanks to its ability to sample a distribution proportional to the exact ground state wave function of a given Hamiltonian. For fermionic systems, the antisymmetric nature of the wave function and its consequent nonpositiveness are usually managed within the fixed node approximation. This implies the introduction of a bias known as nodal error. As energy ϵ is considered, the nodal error $\Delta\epsilon$, which disappears if the nodal surfaces of the exact wave function are known, has a value that commonly spans the range $\Delta\epsilon/\epsilon \in [10^{-5},10^{-4}]$ [21].

In the first part of this paper we will focus on the ideas necessary to extract scattering information from a QMC simulation. In this respect this work can be regarded as complementary to Ref. [19], where more emphasis was put on the explanation of the QMC technique. After that we will show the results of the application of the reviewed method to the elastic collision of Ps on H and He. We will end the paper by discussing some technical topics concerning the computation of annihilation properties in a QMC framework and applications to related area of physics.

II. REVIEW OF THE METHOD

The first suggestions for the application of QMC methods to scattering problems were independently made in two pio-

———————
*Electronic address: Simone.Chiesa@unimi.it
[†]Electronic address: Massimo.Mella@unimi.it
[‡]Electronic address: Gabriele.Morosi@uninsubria.it

neering papers in the context of nuclear physics [22,23]. As already mentioned, those ideas have been recently applied to the exciton-exciton scattering problem [19], thus providing the first accurate calculation for the Ps-Ps system. The main point behind the approach, which closely resembles the R-matrix theory of Wigner and Eisenbud [24], consists in dividing the space around the target into two regions where the problem can be solved exactly (either analytically or computationally). Then the two solutions are matched, requiring the function to have the necessary continuity properties at the boundary. In the following we will explain how to investigate the wave function in these regions and we will point out some issues arising when more particles and higher energies are concerned. Atomic units are used through the paper.

A. Wave function in the external region

Although most of the concepts and equations presented in this section can be easily found in any scattering textbook, we report them here for completness and in order to set up all the definitions we need subsequently. To start, let us define $\mathbf{r}_{AB} = \mathbf{R}_A - \mathbf{R}_B$ as the relative position of the centers of mass of the two composite fragments A and B, p as their asymptotic relative momentum, and $\mu = m_A m_B / (m_A + m_B)$ as their reduced mass. We introduce a boundary surface at $r_{AB} = \mathcal{R}$, where $\mathcal{R}$ satisfies the condition $V(\mathcal{R}) \ll p^2 / 2\mu$, $V(r_{AB})$ being the interaction energy between the two fragments at large center of mass distances. The exact wave function in the region $r_{AB} > \mathcal{R}$ can then be written as

$$\Psi = \mathcal{A}\left[\Psi_A(\mathbf{s}_A)\Psi_B(\mathbf{s}_B)\frac{\Phi_l(r_{AB})}{r_{AB}}Y_{lm} \right] \quad (1)$$

where $\mathcal{A}$ is the antisymmetrization operator, $\mathbf{s}_A$ and $\mathbf{s}_B$ the internal coordinates of the two separate fragments, Ψ_A and Ψ_B their internal wave functions, and Φ_l and Y_{lm} the radial and angular functions describing the dynamics of the relative motion of the two centers of mass (l and m are the usual angular momentum quantum numbers). The stationary form of $\Phi_l(r_{AB})$ can be expressed as

$$\Phi_l(\mathbf{r}_{AB}) = \mathcal{I}_l(pr_{AB}) + S_l(p)\mathcal{O}_l(pr_{AB}) \quad (2)$$

where $\mathcal{I}_l$ and $\mathcal{O}_l$ are Hankel functions, and $S_l(p)$ is the scattering matrix. Here, p is connected to the total energy by

$$E = \frac{p^2}{2\mu} + E_A + E_B, \quad (3)$$

where E_A and E_B are the ground state internal energies of A and B. Both of them can be computed employing the DMC method. Function (2) is the general solution of the radial Schrödinger equation for $r_{AB} > \mathcal{R}$

$$\left[\frac{d^2}{dr^2} - \frac{l(l+1)}{r^2} - p^2 \right]\Phi_l = 0 \quad (4)$$

which, being a linear second order differential equation, admits a unique solution (apart from an unphysical multiplica-

tive constant) once the logarithmic derivative at a given point is specified. Imposing the condition

$$\frac{\Phi_l'(\mathcal{R})}{\Phi_l(\mathcal{R})} = \frac{1}{\mathcal{B}} \quad (5)$$

one has, from Eq. (2), the following expression for the scattering matrix:

$$S_l(p) = -\frac{\mathcal{B}\mathcal{I}_l'(p\mathcal{R}) - \mathcal{I}_l(p\mathcal{R})}{\mathcal{B}\mathcal{O}_l'(p\mathcal{R}) - \mathcal{O}_l(p\mathcal{R})}. \quad (6)$$

It is worth noticing that so far the value of p (and hence E) has been completely arbitrary.

B. QMC solution in the internal region

When the boundary condition (5) is imposed on functions in the interior of the sphere, the solution of the Schrödinger equation is expected to be quantized. E is no longer arbitrary and depends on the specific form of the interaction between the two fragments. The $\mathcal{N}$th energy level turns out to be a function of $\mathcal{B}$ and $\mathcal{R}$, i.e., $E(\mathcal{N}, \mathcal{B}, \mathcal{R})$, and its substitution in Eq. (3) yields a corresponding value for the momentum $p(\mathcal{N}, \mathcal{B}, \mathcal{R})$. This last quantity gives, thanks to Eq. (6), the desired value of $S_l(p)$. Thus, given a method to compute E in the interior, controlling the boundary condition, the scattering problem can be considered solved. Cast in this way, the problem involves the energy computation of a confined system and is therefore suited for a QMC study. The possibility of varying E by changing $\mathcal{N}$, $\mathcal{B}$, and $\mathcal{R}$ can be fully exploited in a variational Monte Carlo simulation thanks to the ease of controlling the value of $\mathcal{B}$. Contrariwise, in DMC simulations like those we have employed in this work, one is essentially forced to the choice $\mathcal{B} = 0$. From a physical point of view, this corresponds to seeking for the eigenstates of a system enclosed in a rigid sphere with radius $\mathcal{R}$ centered on the target. Thus, exploiting the definition of the phase shift $\delta_l(p)$, $S_l = e^{2i\delta_l}$, recalling the relation between Bessel (j_l), Neumann (n_l), and Hankel functions

$$\mathcal{I}_l = j_l + in_l,$$

$$\mathcal{O}_l = j_l - in_l, \quad (7)$$

and setting $\mathcal{B} = 0$, one can easily rearrange Eq. (6) as

$$\tan\delta_l(p) = -\frac{j_l(p\mathcal{R})}{n_l(p\mathcal{R})}. \quad (8)$$

Equation (3) of Ref. [19] is a more approximate formula for the computation of δ_l that coincides with ours only when $l = 0$. In testing the DMC approach to the scattering calculation of a positron off a model spherical potential and the H atom with $l \geqslant 0$ [25], we found Eq. (8) to be far more accurate than the expression previously cited. For the case $l = 0$, Eq. (8) assumes the particularly simple form

$$\tan\delta_0(p) = -\tan p\mathcal{R} \quad (9)$$

and hence

$$\delta_0 = \mathcal{M}\pi - p\mathcal{R}, \tag{10}$$

where $\mathcal{M}$ can be any integer. Because of our interest in low energy processes, we only performed s-wave simulations using Eq. (10) for the computation of the phase shifts and a value of p provided by Eq. (3). As shown in Ref. [19], if one identifies $\mathcal{M}$ with the label of the internal state under consideration (which we called $\mathcal{N}$), δ_l becomes a continuous function of p whose behavior in the limit $p \rightarrow 0$ agrees with Levinson's theorem.

C. Excited states and nodes

Before going on, it is worth stressing a few important points. First, while an upper limit to the sphere radius $\mathcal{R}$ does not exist, it cannot be chosen smaller than some unspecified threshold value. This is due to the required validity of Eq. (1) everywhere outside the sphere and imposes an upper limit to the relative kinetic energy. In the case of Ps scattering off neutral atoms, the interaction potential between the target and the projectile decays as $1/r_{AB}^6$, allowing the use of fairly small radii, a possibility not necessarily available for different colliding fragments. Second, since DMC is mainly a ground state technique, its straightforward application to situations where projectile and target can form a bound state seems prevented. If it were used, the method would end up sampling the wave function of the global ground state, which does not carry information about scattering processes. To tackle and overcome these issues, one has to employ an orthogonalization procedure able to retrieve information from the excited states. This gives the possibility of raising the energy while keeping the boundary constraint fixed and, in principle, would allow the study of systems at any energy. To realize that, following the work previously done in Ref. [19], we employed the correlated function DMC (CFDMC) method [26], which combines the action of the projection operator typical of a normal DMC simulation with the use of a basis set of N many-body wave functions. The algorithm projects these N functions on the first N states of the Hamiltonian. An example of that is given in Fig. 1 which displays the action of the projection operator on the first four states of the Ps-H singlet as energy decay in imaginary time. In this specific case the system has an overall bound state, and therefore scattering information can be retrieved only from the second level on. For the sake of clarity we would like to specify that, in the following, results for Ps-He and Ps-H triplets, which do not have any bound states, were computed without employing the CFDMC method.

Although a detailed description of this method is out of the scope of the present work and can be extensively found in the literature [26,27], we would like to comment on a few features connected to the presence of nodes. The source of nodal surfaces is threefold. First, a radial nodal surface located at $r_{AB} = \mathcal{R}$ is introduced by the spherical confining potential that allows the scattering problem to be recast into a bound state one. This is always present in any of the N basis functions as well as in the projected states. As immediate consequence of this, one can apply Eq. (10) to calculate
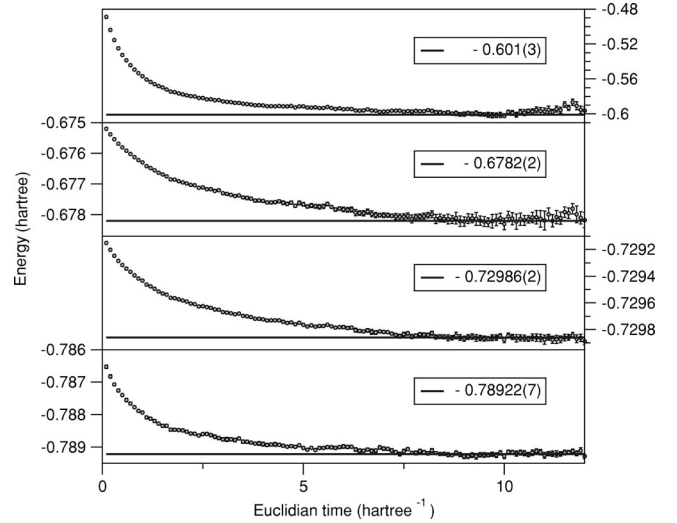

FIG. 1. Energy (hartree) decay versus the elapsed time t (Hartree^{-1}) for the first four states of the Ps-H system with $S=0$ and $\mathcal{R}=15$ a.u. Note the different energy scales on each plot and their relative shifts. Also, note that the energy of the ground state is correctly less than -0.75 and coincident with that of the bound state of Ps-H. The numbers and thick lines in each plot represent the asymptotic value of the energy for that state as computed by averaging over the last 2–3 Hartree^{-1} of the decay curves.

phase shifts. Second, there are "almost spherical" nodes introduced into $\Phi_l(r_{AB})$ to describe a Ps projectile with higher kinetic energy in a state orthogonal to the ground state of the enclosed target-projectile system. Third, there are nodal surfaces generated by the use of the appropriate antisymmetrizer $\mathcal{A}$ (or the correct exchange operator $\mathcal{O}$ in a spin-free formalism). These are needed to prevent bosonic collapse of the Ps electron on the target and to correctly account for the target state symmetry. On the basis of the Young's tableau, the $\mathcal{O}$ operator for the A-Ps system could be obtained by acting on the symmetry operator $\mathcal{O}_A$ of the target with $\Pi_i(1 - \mathcal{P}_{iPs})$ [28]. Here, $\mathcal{P}_{iPs}$ is the exchange operator between the Ps electron and the target electron i of equal spin. This operation changes the location of the nodal surfaces (if any is present) in the "target" region by an extent that is somehow related to the confining sphere radius $\mathcal{R}$. If no overall bound state between the target and the projectile exists, so that the CFDMC method is not in principle needed to extract low energy results, the dependency on $\mathcal{R}$ comes simply from the fact that it implicitly defines the "localization" of the Ps around the target. The larger $\mathcal{R}$ the lower the Ps electron density in the target region. In an independent particle approach, the contribution of $\mathcal{P}_{iPs}$ from $1 - \mathcal{P}_{iPs}$ in defining the target nodes depends on the local Ps electron amplitude, a contribution that decreases upon increasing the sphere radius. In turn, this indicates a vanishing effect on the energy, and hence on the $\delta(p)$, of the exchange between the Ps electron and the target ones. These conclusions are identical for every one of the N projected states in the CFDMC procedure, and also if correlation effects between the particles are introduced. In addition, the $\Pi_i(1 - \mathcal{P}_{iPs})$ exchange introduces a nodal surface on the periphery of the target electron density that we expect to resemble a sphere for large $\mathcal{R}$. This is due to the decreas-

ing importance of details in the Ps-*A* interaction when the sphere becomes larger. This is exactly the case for Ps-H and Ps-He scattering where no internal target nodes are present. In the case of a global Ps-*A* bound state (e.g., Ps-Li, the smallest system having a target with internal nodal surface), this picture is complicated by the fact that the nodes in the ground state wave function may be quite different from the ones in the excited (scattering) states. However, the usage of a guiding function that has nonzero overlap with all the *N* computed states in the CFDMC approach, and that prevents bosonic collapse of the sampled electron distribution, assures the correctness of the procedure, allowing the correct mixing and projection of the starting *N* basis set functions. Nevertheless, it should be stressed that the efficiency of such a procedure may strongly depend on the quality of the chosen guide function. However, the fixed nodes approximation can have dramatic effects when inelastic and reactive processes are considered. In these cases the structure of the wave function changes abruptly in a way that must be similar to what happens when, in a bound system, one considers two different electronic states. As far as we know, little can be said about the change of nodal structure on going from the ground state to an electronic excited state where more than two electrons are involved. We finally remark that the orthogonality between states with different global angular momentum ensures that every projected state will have the same angular symmetry of the guiding function.

III. APPLICATIONS

In this work, we applied the presented technique to the *S*-wave scattering of positronium off hydrogen and helium. A historical description of how calculations for these systems have evolved so far can be found in reference [29] and [30]. The dynamics of both systems was characterized by the full Hamiltonian

$$H = -\frac{1}{2}\sum_{i=1}^{N_e}\nabla_i^2 - \frac{1}{2}\nabla_p^2 - \sum_{i=1}^{N_e}\frac{Z}{r_i} + \frac{Z}{r_p} + \sum_{i>j}\frac{1}{r_{ij}} - \sum_i^{N_e}\frac{1}{r_{ip}},$$

(11)

where *i* and *j* refer to electrons, *p* to the positron, and *Z* to the nuclear charge of the atom. In order to reduce the statistical error associated with our energy results, we importance-sampled using a guiding wave function whose spatial part has the form

$$\Psi = \mathcal{O}\left[\Psi_A(\mathbf{s}_A)\Psi_{Ps}(r_{1p})\frac{\Phi(r_{PsA})}{r_{PsA}}\phi_J(\mathbf{s}_I)\right],$$

(12)

where ψ_A, ψ_{Ps}, and Φ have the same meaning as in Eq. (1). ϕ_J is a Jastrow factor for all the pairs of particles belonging to different fragments, $\mathbf{s}_I$ is the set of distances for these pairs, and $\mathcal{O}$ is the appropriate symmetry operator built according to Young's diagrams. To make the function vanishing on the sphere surface, $\Phi(r_{PsA})/r_{PsA}$ was chosen to be a linear combination of polynomials of the form

$$\frac{\Phi_l(r_{AB})}{r_{AB}} = \sum_k a_k(r_{PsA}^2 - \mathcal{R}^2)^2,$$

(13)

which allows one to reduce the cost of evaluating the guiding function. In the simulation reported in this work, $\mathcal{R}$ has been varied from a minimum of 10 to a maximum of 50 bohr. Also, as is common practice in DMC calculations, in all simulations we chose the trial wave function coincident with the guiding function, and we set the values of the parameters a_k to avoid local energy divergencies on the sphere surface. This is important in order to prevent population blowup and to reduce the statistical error of the energies.

A. Hydrogen

In the Ps-H case, the exact internal wave function of both fragments is known and $\mathcal{O}$ has the form

$$\mathcal{O} = 1 + (-1)^S P_{12},$$

(14)

where *S* is the electronic spin angular momentum of the state (0 or 1) and P_{12} the permutation operator between the two electrons. The space part of the $S=0$ ground state function is everywhere positive, while the nodal surface for the $S=1$ state is exactly provided by the action of $\mathcal{O}$. This comes from the space symmetry of the state, which dictates that the wave function be dependent only on the interparticle distances, and by recognizing that the presence of the positron does not introduce any modification to the location of the nodal surface for a two-electron system, namely, $r_1 = r_2$ [31]. Under this condition the energy can be computed by DMC simulation without any nodal approximation.

All the simulations for the triplet state of Ps-H were carried out using a time step of 0.01 Hartree^{-1}, 2000 walkers, and a total of 100 blocks of 10 000 steps each.

The singlet state, which supports a bound state, has been studied exploiting the CFDMC technique. It is worth recalling that the bound state energy for this system has already been computed using DMC simulation [32]. The obtained value of $-0.789\,175(10)$ a.u. agrees well with the very accurate estimate of $-0.789\,196\,714\,7(42)$ a.u. computed by Yan and Ho [33]. As trial functions for the excited states we employed expressions identical to Eq. (12) with the choice

$$\Phi(r_{Ps\text{-}H}) = \sin\left(\frac{n\pi r_{Ps\text{-}H}}{\mathcal{R}}\right).$$

(15)

The trial function for the ground state was instead chosen to be

$$\Psi_{Ps-H} = \mathcal{O}\exp\left[\frac{\alpha_1 r_1 + \alpha_2 r_1^2}{1+\alpha_3 r_1} + \frac{\beta_1 r_2 + \beta_2 r_2^2}{1+\beta_3 r_2} + \frac{\gamma_1 r_p + \gamma_2 r_p^2}{1+\gamma_3 r_p}\right.$$
$$\left. + \frac{\zeta_1 r_{12}}{1+\zeta_2 r_{12}} + \frac{\mu_1 r_{1p}}{1+\mu_2 r_{1p}} + \frac{\nu_1 r_{2p}}{1+\nu_2 r_{2p}}\right],$$

(16)

a form already employed in the context of ground state calculations [20]. Simulations for the singlet states were per-
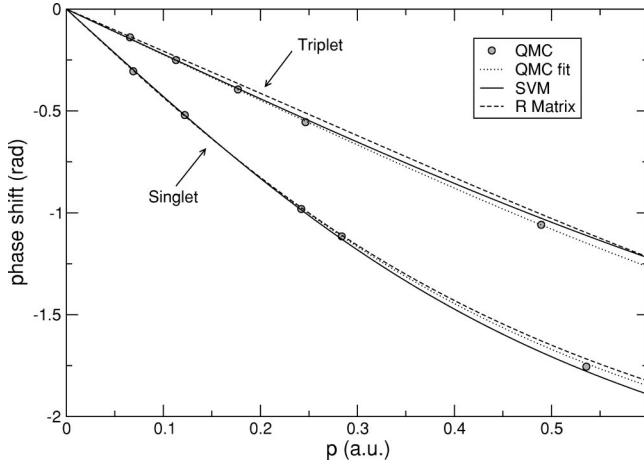
FIG. 2. S-wave elastic phase shift for H with total electron spin $S=1$ and $S=0$. The momentum is expressed in atomic units.

formed employing 2000 configurations, a time step of 0.01 Hartree^{-1}, and a grand total of 10 000 decorrelated Euclidean time evolutions.

Low energy phase shifts for both $S=0$ and $S=1$ systems are shown in Fig. 2 where they are directly compared to the fitting results from stochastic variational minimization (SVM) [14] and R-matrix [17] calculations. A summary of other estimates is reported in Table I. The scattering lenghts a_s were calculated by fitting the effective range formula

$$p \cot \delta(p) = -\frac{1}{a_s} + \frac{1}{2}rp^2 \qquad (17)$$

to the computed phase shifts. A fitting of the five points obtained for the singlet leads to $a_s=4.357(28)$ a.u. and $r=2.259(39)$ a.u. However, because the phase shift associated with the highest momentum lies in a region that could be outside the range of applicability of Eq. (17), we consider the value $a_s=4.375(34)$ a.u. a more reliable estimate. This value (to which we will refer in the following, if not otherwise specified) was obtained by excluding the highest momentum point from the fitting procedure. The effective range for this fit is $r=2.228(50)$ a.u. Our value differs equally from those proposed by Ivanov, Mitroy, and Varga [14] (hereafter cited as IMV) and Blackwood, McAlinden, and Walters [17] (cited as BAW) by about 0.8%. In their paper BAW suggest that the SVM value of IMV was probably closer to the correct one. Unfortunately, the standard devia-

TABLE I. Scattering length (a.u.) for the Ps-H scattering system with total spin $S=0$ and $S=1$.

	QMC	Other
$S=0$	4.375(34)	4.34 [a], 3.49 [b], 4.41 [c], 4.5 [d]
$S=1$	2.246(21)	2.22 [a], 2.46 [b], 2.06 [c]

[a]Reference [14], stochastic variational minimization.
[b]Reference [13], Kohn variational method.
[c]Reference [17], 14Ps14H R-matrix calculation.
[d]References [2,3], stabilization calculations.

tion associated with our value of a_s makes it impossible to single out which of these two estimates is the more accurate. Moreover, the overall agreement between these three techniques seems to definetely rule out the value proposed in [13]. Indeed, it was already suggested [17,14] that truncation in the expansion used to evaluate the matrix elements in Ref. [13] could have led to erroneous results in the Kohn variational approach [34].

The corresponding values for the triplet state are $a_s=2.246(21)$ a.u. and $r=1.425(43)$ a.u. The agreement between this value of a_s and the value of IMV is of the order of 1% whereas that of BAW lies 10% lower than ours. At the moment we do not understand the origin of this fairly large difference. In principle, the DMC method applied to this system has virtually no errors. Nodal surfaces are exactly provided and the time step bias is negligible because of the smallness of the step size. The large value of box radius employed for points at low energy (50, 40, and 30 bohr) makes us confident about the validity of approximation (1) and the correctness of the fit from which we determine a_s. Finally, the statistical accuracy we reached excludes possible differences due to the uncertainty in the location of our phase shift. On the other hand, the values computed by BAW can be affected by the truncation of the basis set and the Buttle correction approximation consequently introduced. Values seems to be well converged but it is well known that the inclusion of certain configurations or of a different kind of basis function can have dramatic effects on many physical properties [35].

Before discussing the results for Ps-He, we would like to stress that the observed agreement between completely different computational techniques, like the QMC, SVM, and, even if to lower extent, R-matrix methods, can be considered as strong evidence for the correctness of the results proposed, as well as a strong proof of the reliability of the method. Also, it is interesting to notice that, although quite dated, the results by Drachman and Houston [2,3] were very close to the DMC and SVM results.

B. Helium

With this premise, we now address the more debated problem of positronium scattering off helium. Before discussing our computed quantities for this process, it is worth noting that the experimental measurements of the threshold value of the cross section span almost an entire order of magnitude [8,11]. The most recent theoretical estimates, obtained by different computational schemes and reported in Table II, do not single out one of these experimental results as the correct one. The primary reason for this failure is the small size of the cross section and the consequent large fractional error associated with any approximation.

In the present study, the system is treated with a genuinely many-body technique and no physical approximations have been made prior to the numerical simulation. The absolute freedom one has in choosing the analytical form of the wave function in QMC methods allows us to employ the following explicitly correlated form for Ψ_{He}:

TABLE II. Scattering threshold cross section (π a.u.) for the Ps-He scattering system.

QMC	Experiment	Other
7.8916(67)	8.4(9) [a], 8(1) [b]	10.56 [f], 9.83 [f]
	13(4) [c], 9.0 [d]	8.79 [f], 3.10 [g]
	2.6(5) [e]	13.2 [h], 11.9 [i], 7.40 [j]

[a]Reference [7], Canter *et al.* (1975).
[b]Reference [37], Rytsölä *et al.*(1984).
[c]Reference [8], Nagashima *et al.*(1998).
[d]Reference [9], Coleman *et al.*(1994).
[e]Reference [11], Skalsey *et al.*(1998).
[f]Reference [18], frozen-core stochastic variational minimization.
[g]Reference [15], three-state close coupling with model exchange.
[h]Reference [16], 22-state *R*-matrix calculation.
[i]Reference [4], Kohn variational method with model exchange.
[j]Reference [39], 2Ps3He *T*-matrix calculation.

$$\Psi_{He} = \exp\left(\frac{\alpha_1 r_1 + \alpha_2 r_1^2}{1 + \alpha_3 r_1} + \frac{\beta_1 r_2 + \beta_2 r_2^2}{1 + \beta_3 r_2} \right.$$
$$\left. + \frac{\gamma_1 r_{12}}{1 + \gamma_2 r_{12}} \right), \tag{18}$$

which gives a statistically exact DMC energy. Here, we forced $\alpha_1 = \beta_1 = -2$ and $\gamma_1 = 1/2$ to exactly satisfy the cusp conditions of the ground state wave function. This choice helps in reducing the stochastic noise of our results, and in preventing explosions in the walker population during the simulations. Using this trial wave function to guide the simulations and to compute the total energy, we found the DMC energy to be statistically equal to the exact value 2.903 724 377 0 a.u. [36] for time steps ranging from 0.001 Hartree^{-1} to 0.03 Hartree^{-1}.

Moreover, the only Young diagram compatible with the choice of a helium atom in its ground state ($S=0$) gives the following form for $\mathcal{O}$:

$$\mathcal{O} = (1 + P_{12})(1 - P_{13}). \tag{19}$$

Simulations for this system were characterized by a time step of 0.005 Hartree^{-1}, 4000 walkers, and a total of 130 blocks of 25 000 steps each.

Each value of p has been computed by subtracting from the DMC energy the Ps internal energy and the helium energy specified above. This last quantity is far more accurate than our error bars. The value of the scattering length, obtained by linear fitting $\delta(p)$ versus p (Fig. 3), is 1.4046(6) a.u. with a corresponding threshold cross section of 7.8916(67)π a.u.

The best agreement with experimental data is found with the scattering threshold cross section of 8(1)π a.u. proposed by Rytsölä *et al.* [37] and the measure of 8.4(9)π a.u. performed by Canter *et al.* [7]. These values are reported in Table II with a list of other experimental values. As was already pointed out in Ref. [18], the estimate of Skalsey *et al.* [11] (2.5π a.u.) was performed at an energy too high to be relevant to this work. In order to thoroughly assess the
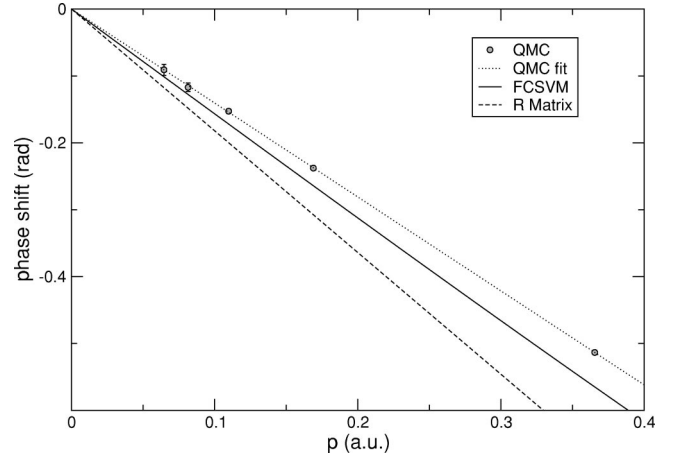

FIG. 3. *S*-wave elastic phase shift for He with total electron spin $S = 1/2$. The momentum is expressed in atomic units.

quality of our results, a discussion of the other computational methods is mandatory. In Ref. [16], an *R*-matrix 22-Ps-pseudostate calculation gave 13.2π a.u., employing a single state to represent He (see Fig. 3). This was chosen to be the Hartree-Fock quality wave function by Clementi and Roetti [38], hence not containing intraatomic correlation. While the 22-Ps-pseudostate basis set could be regarded as accurate in dealing with Ps excitation and distortion, the lack of excitations in the He target, which are expected to "soften" the Ps-He interaction analogously to what happens in Ps-H, is probably the reason for the larger cross section with respect to the QMC one. As to the results from Refs. [14] and [18], they were obtained by means of a frozen-core variant of the SVM method, the unique difference being the parametrization of the core polarization potential. When no polarization was used, the resulting cross section (13.56π a.u.) is in accurate agreement with the *R*-matrix 22-Ps-pseudostate calculation, indicating the consistency of the two procedures. Upon introducing the polarization potential, a decrease of the cross section is obtained, as expected from the less repulsive Ps-He interaction. The extent of the decrease was also found to be dependent on the way the parametrization of the polarization potential was carried out. More specifically, Mitroy and Ivanov [18] found a Ps-He threshold cross section of 10.56π a.u. when this potential was tuned to reproduce the electron-He phase shift, whereas a value of 8.79π a.u. was obtained when the parametrization was chosen to coincide with the positron-He case. As expected, using a parametrization that averages between the two potentials gave a cross section of 9.83π a.u. This value, which we consider the fairest estimate in the theoretical framework of Ref. [18], has been used to represent the SVM curve in Fig. 3. Although the extent of the changes is relatively small, in our view these results highlight some sensitivity of the threshold cross section with respect to the correlation between the internal structure of the two fragments. The *K*-matrix approach of Basu *et al.* [39] is, to the best of our knowledge, the only calculation explicitly dealing with excitations of He. Passing from a 3Ps1He basis set to a 2Ps3He one, they observed a decrease in the threshold cross section from 14.75π a.u. (in good agreement with the 22Ps1He *R*-matrix calculation and

the frozen-core SVM calculation without polarization potential) to 7.40π a.u. Although these basis sets are rather incomplete and some (not assessed) approximation was introduced [18], this drop may testify the importance of a correct description of He and how this systematically drives the cross section toward a lower value. As to the result from Ref. [15], this was obtained using a model exchange potential whose parametrization was carried out using a rather incomplete basis set to reproduce the electron phase shift. Also, as previously found for Ps-H, the result by Drachman and Houston [4], 7.73π a.u., obtained by means of a Kohn variational approach with fixed exchange, shows an uncannily good agreement with the DMC estimate, being the closest among all the other values.

At this time, the nodal error, being the only approximation introduced, deserves some comments. As a consequence of the fixed node approximation, the energy is an upper bound to the exact one, their difference being dependent on the quality of the chosen nodal surfaces. General considerations [40] show this bias in the phase shift to be always negative and proportional to $\mathcal{R}^{-1}$. As a result of this, our scattering length might be slightly lower than the exact one. More quantitatively, one can observe that in the interaction region (which one can define as a sphere of radius $\mathcal{R}_I$) the employed function closely resembles the functional form used in bound state calculations on similar systems, for which the nodal error roughly equals $\Delta \epsilon_B = 1 \times 10^{-4}$ Hartree [20]. In the rest of the simulation volume the nodes of the trial wave function are essentially exact because of the validity of Eq. (1). For this reason we expect a bias on the energy [40] of the order of $\Delta \epsilon = \Delta \epsilon_B \mathcal{R}_I / \mathcal{R}$. If so, the nodal error would turn out to be of the same order of magnitude as the statistical fluctuations of our energy values, roughly 3×10^{-5} Hartree. These considerations thus indicate the statistical exactness (between 2 or 3 times the statistical error bar) of our results.

IV. CONCLUSION AND FUTURE DEVELOPMENTS

The DMC and CFDMC methods have been used to obtain scattering lengths and threshold cross sections for Ps scattering off H and He. As to the H target, our results for both the singlet and triplet states are found to be close to coincidence with the SVM ones by Ivanov *et al.* [14], and really close to the R-matrix 14Ps14H pseudostate ones [12]. As far as He is concerned, the fixed node DMC value for the cross section is found in fair agreement with the frozen-core SVM ones when polarization potentials are used, and is proposed as the most accurate estimate of this quantity.

Among the results directly derivable from this method,

we would like to emphasize that the possibility of sampling the exact particle distributions in configurational space (employing, for example, the forward walking algorithm [41] or the reptation method [42]) could allow one to obtain an effective interaction potential between Ps and a given atom or molecule. This potential, where all the physical effects are correctly accounted for, could be subsequently used to simulate Ps in condensed phases such as molecular crystals and liquids, relying on the pair approximation to define the total interaction potential. Moreover, this study could also help in defining preferential spatial locations where the Ps positron would annihilate during a "pick-off" annihilation event. So the interplay between the theoretical and the experimental results may enhance the diagnostic role played by Ps in condensed matter science. As already pointed out in the Introduction, one of the issues in the positron field is the computation of annihilation properties of the target. In the context of positron scattering the central quantity is the effective charge Z_{eff}. This quantity is expressed by

$$Z_{\text{eff}} = \left\langle \Psi \left| \sum_i \delta(r_{ip}) \right| \Psi \right\rangle, \quad (20)$$

where r_{ip} is the distance between the positron and the ith electron, and Ψ is the scattering wave function normalized in order to describe a unitary flux of incident positrons. We recently proposed an algorithm [43] to deal formally with the same integral, but in the case of a bound system [in that context the integral (20) is proportional to the annihilation rate]. In those circumstances, the wave function needed to be normalized, as in any bound state, in order to describe a probability density. The same technique of Ref. [43] can thus be applied provided one introduces a correction of the value obtained for a proper normalization integral [44]. The extension of this procedure to estimate $^1Z_{\text{eff}}$ should be straightforward, at least for closed shell targets [45]. We conclude by remarking again that the extension to reactive processes is feasible (the formalism has been known since the seminal works of Alhassid and Koonin [22], and Carlson *et al.* [23]), but it seems to contain uncontrolled approximations when the use of the fixed node CFDMC method is required.

[1] O.E. Mogensen, *Positron Annihilation in Chemistry* (Springer-Verlag, Berlin, 1995).

[2] R.J. Drachman and S.K. Houston, Phys. Rev. A **12**, 885 (1975).

[3] R.J. Drachman and S.K. Houston, Phys. Rev. A **14**, 894 (1976).

[4] R.J. Drachman and S.K. Houston, J. Phys. B **3**, 1657 (1970).

[5] B.A.P. Page, J. Phys. B **9**, 1111 (1976).

[6] P.A. Fraser, J. Phys. B **1**, 1006 (1968).

[7] K.F. Canter, J.D. McNutt, and L.O. Roellig, Phys. Rev. A **12**, 375 (1975).

[8] Y. Nagashima, T. Hyodo, F. Fujiwara, and A. Ichimura, J. Phys. B **31**, 329 (1998).

[9] P.G. Coleman, S. Rayner, F.M. Jacobsen, M. Charlton, and

R.N. West, J. Phys. B **27**, 981 (1994).

[10] A.J. Garmer, G. Laricchia, and A. Özen, J. Phys. B **29**, 5961 (1996).

[11] M. Skalsey, J.J. Engbrecht, R.K. Bithell, R.S. Vallery, and D.W. Gidley, Phys. Rev. Lett. **80**, 3727 (1998).

[12] C.P. Campbell, M.T. McAlinden, F.G.R.S. MacDonald, and H.R.J. Walters, Phys. Rev. Lett. **80**, 5097 (1998).

[13] S.K. Adhikari and P. Mandal, J. Phys. B **34**, L187 (2001).

[14] I.A. Ivanov, J. Mitroy, and K. Varga, Phys. Rev. Lett. **87**, 063201 (2001); Phys. Rev. A **65**, 032703 (2002).

[15] P.K. Biswas and S.K. Adhikari, Phys. Rev. A **59**, 363 (1999).

[16] J.E. Blackwood, C.P. Campbell, M.T. McAlinden, and H.R.J. Walters, Phys. Rev. A **60**, 4454 (1999).

[17] J.E. Blackwood, M.T. McAlinden, and H.R.J. Walters, Phys. Rev. A **65**, 32517 (2002).

[18] J. Mitroy and I.A. Ivanov, Phys. Rev. A **65**, 012509 (2002).

[19] J. Shumway and D.M. Ceperley, Phys. Rev. B **63**, 165209 (2000).

[20] M. Mella, G. Morosi, and D. Bressanini, J. Chem. Phys. **111**, 108 (1999).

[21] A. Luchow and J.B. Anderson, Annu. Rev. Phys. Chem. **51**, 501 (2000).

[22] Y. Alhassid and S.E. Koonin, Ann. Phys. (N.Y.) **155**, 108 (1984).

[23] J. Carlson, V.R. Pandharipande, and R.B. Wiringa, Nucl. Phys. A **424**, 47 (1984).

[24] E.P. Wigner and L. Eisenbud, Phys. Rev. **72**, 29 (1947).

[25] S. Chiesa and M. Mella (unpublished). Our test on positron scattering off H indicates that the DMC approach agrees accurately with the results of more standard calculation methods.

[26] D.M. Ceperley and B. Bernu, J. Chem. Phys. **89**, 6316 (1988).

[27] F.V. Prudente, L.S. Costa, and P.H. Acioli, J. Phys. B **33**, R285 (2000).

[28] Depending on the chosen total spin state, the correct symmetry operator should actually contain also the action of (1 $+ \mathcal{P}_{kPs}$), where k is the first unsymmetrized target electron having opposite spin to the Ps one.

[29] H.R.J. Walters, J.E. Blackwood, and M.T. McAlinden, in *New Directions in Antimatter Chemistry and Physics*, edited by C.M. Surko and F.A. Gianturgo (Kluwer Academic, Dordrecht, 2001).

[30] A.S. Ghosh and P.K. Sinha, in *New Directions in Antimatter Chemistry and Physics* [29].

[31] D. Bressanini, D.M. Ceperley, and P.J. Reynolds, in *Recent Advances in Quantum Monte Carlo Methods, II*, edited by S.T. Rothstein (World Scientific, Singapore, 2001).

[32] D. Bressanini, M. Mella, and G. Morosi, Phys. Rev. A **57**, 1678 (1998).

[33] Z.C. Yan and Y.K. Ho, Phys. Rev. A **59**, 2697 (1999).

[34] W. Kohn, Phys. Rev. **74**, 1763 (1948).

[35] J.E. Blackwood, C.P. Campbell, M.T. McAlinden, and H.R.J. Walters, Phys. Rev. A **60**, 30502 (2002).

[36] A.M. Frolov, Phys. Rev. A **57**, 2436 (1998).

[37] K. Rytsölä, J. Vettenranta, and P. Hautojärvi, J. Phys. B **17**, 3359 (1984).

[38] E. Clementi and C. Roetti, At. Data Nucl. Data Tables **14**, 177 (1974).

[39] A. Basu, P.K. Sinha, and A.S. Ghosh, Phys. Rev. A **63**, 052503 (2001).

[40] S. Chiesa and M. Mella (unpublished).

[41] B.L. Hammond, W.A. Lester, and P.J. Reynolds, *Monte Carlo Methods in Ab Initio Quantum Chemistry* (World Scientific, Singapore, 1998).

[42] S. Baroni and S. Moroni, Phys. Rev. Lett. **82**, 4745 (1999).

[43] M. Mella, S. Chiesa, and G. Morosi, J. Chem. Phys. **116**, 2852 (2002).

[44] S. Chiesa, M. Mella, and G. Morosi (unpublished).

[45] J. Mitroy and I.A. Ivanov, Phys. Rev. A **65**, 042705 (2002).